J Sol-Gel Sci Technol (2017) 83:64–71
DOI 10.1007/s10971-017-4383-2

ORIGINAL PAPER: NANO- AND MACROPOROUS MATERIALS (AEROGELS, XEROGELS, CRYOGELS, ETC.)

Synthesis and characterization of ambient-dried microglass fibers/silica aerogel nanocomposites with low thermal conductivity

Yonggang Jiang[1] · Junzong Feng[1] · Jian Feng[1]

Received: 9 January 2017 / Accepted: 3 April 2017 / Published online: 19 April 2017

Abstract A new ambient-dried silica aerogel nanocomposites reinforced by smaller diameter microglass fiber mat were synthesized. Effects of gel treatment and drying temperature, molar ratio of modification agent and volume content of microglass fiber on the composites' structure and properties were investigated. Increasing the gel treatment temperature with a gradient multi-segment drying process, the aerogel density and volume shrinkage decreased rapidly. Homogeneous and translucent bulk aerogel could be obtained with the density of 0.129 g/cm^3, specific surface area of 731.76 m^2/g and average pore size of 20 nm. Fewer cracks, more silica matrix and stronger fiber/silica interface, which significantly improves the mechanical performance of the nanocomposites with a high bending strength of 1.4 MPa. The thermal conductivity of the ambient-dried nanocomposites decreased and the bending strength increased with increasing fibers' volume content. The retrieved nanocomposites is an excellent thermal insulation material with lower thermal conductivity (0.022 W/m K, 650 °C) and high mechanical performance.

Graphical Abstract

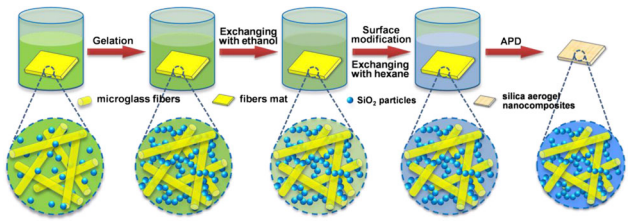

Keywords Silica aerogel nanocomposite · Microglass fibers · Ambient pressure · Thermal conductivity

1 Introduction

In 1931, silica aerogel was firstly prepared by Kistler [1] via a Supercritical Drying (SPD) technology, in an autoclave with an excess of liquid and above the critical temperature. Silica aerogel is a nanostructured material with low thermal conductivity (~0.015 W/m K, 25 °C), low bulk density (~0.03–0.1 g/cm^3) and high specific surface area (~1000 m^2/g). In order to improve the mechanical performance, silica aerogels were reinforced by particles [2–5], whiskers, [6, 7] and fibers [8–15], the SPD-silica nanocomposites with low thermal conductivity and high mechanical performance expands its uses especially when exposed to vibration and compression as an excellent thermal insulation materials [16–20].

However, the SPD processing is expensive, hazardous, restricting the commercial exploitations of silica aerogel nanocomposites [21]. Today, one of the most focusing areas is silica aerogel nanocomposites synthesized via Ambient Pressure Drying (APD) technology to further decrease the manufacturing cost. Recently, the APD-silica aerogel nanocomposites were reported and reinforced by particles [22–27], nanotubes [28], foams [29, 30], and fibers (including cotton)

✉ Yonggang Jiang
jygemail@163.com

[1] Science and Technology on Advanced Ceramic Fibers and Composites Laboratory, National University of Defense Technology, Changsha Hunan 410073, People's Republic of China

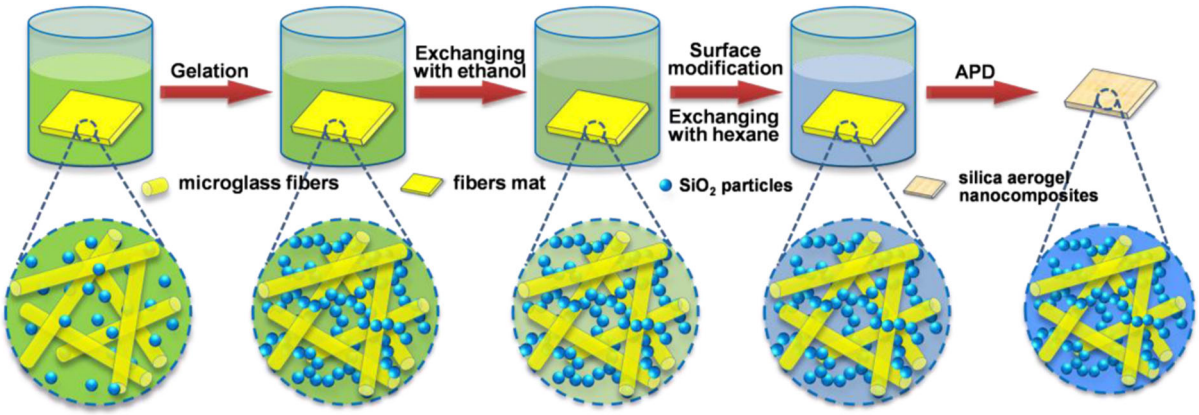

Fig. 1 Schematic overview of ambient-dried microglass fibers/silica aerogel nanocomposites

[31, 32], aramid fibers [33, 34], polyester fibers [35], non-woven fibers [36], glass wool [37], aluminosilicate glass fiber [38], silica fibers [39], mullite fibers [40], glass fibers [41–44], carbon fibers [45, 46], and boehmite nanofiber [47]. For example, Liu GW [40] demonstrated the super insulation mullite fiber/silica aerogel nanocomposites with low thermal conductivity (500 °C, 0.0393 W/m K) and good mechanical property (storage modulus of 12.5 MPa) in 2016.

For the surface modification and drying procedure as reported in all above APD-silica aerogel nanocomposites papers, the wet silica gels were commonly immersed into a modification agent (such as trimethylchlorosilane (TMCS)/n-hexane) by constant volume ratio to make the gels hydrophobic, and were dried slowly at ambient pressure. It is reported that the solvent-modification agents molar ratio [48–50] and drying temperature ramp [31, 51, 52] had a significant effect on the APD-silica aerogel, and fiber diameter had a significant effect on the radiative conductivity of fibrous materials [53]. But the effects of gel treatment and drying temperature, modification agent molar ratio on the APD-silica aerogel nanocomposites reinforced by smaller diameter fibers had received little attention. In this paper, we report a new ambient-dried silica aerogel nanocomposites reinforced by smaller diameter microglass fiber mat, as-prepared nanocomposites have a lower thermal conductivity and high mechanical performance, their effects of gel treatment and drying temperature, modification agent molar ratio and microglass fibers volume content on the composites structure and properties were investigated.

2 Experimental

2.1 Materials

Tetraethoxysilane (TEOS), ethanol (EtOH), n-hexane, hexamethyldisilazane (HMDZ), hydrochloric acid (37%), and ammonia (27%) were obtained from Sinopharm Chemical Reagent Co., Ltd. (Sinopharm, China). Deionized water was used to prepare HCl (aq) and $NH_3{\cdot}H_2O$ (aq) which were used as the acid and base catalysts, respectively. The glass fiber used in this research was microglass fiber mat (Sinoma, Nanjing, China), with the fiber diameter of 2–4 μm and thermal conductivity of 0.036 W/m K at room temperature.

2.2 Synthesis of ambient-dried microglass fibers/silica aerogel nanocomposites

Silica alcogel was synthesized by two step (acid–base) Sol–Gel Process [10]. Figure 1 illustrated the schematic overview of ambient-dried microglass fibers/silica aerogel nanocomposites. Firstly, the microglass fiber mat was immersed into the silica sol in vacuum. Microglass fibers volume content (f_c) was controlled with 4.5, 6.8, and 9.1%, respectively. After gelation, the fiber/gels were washed in EtOH twice in 24 h in order to exchange pore water and also strengthen the network of the gels. The slylation of wet fiber/gels was carried out by immersing into a HMDZ/n-hexane silylating agent solution (25% HMDZ in n-hexane) for 4 times in 96 h. Finally, surface modified wet fiber/gels were exchanged in n-hexane twice in 24 h in order to remove the unreacted silylating agent, and dried at ambient pressure at high temperature (see Table 1, Drying programmer) controlled by gradient multi-segment programmers' oven, evaporating the trapped solvent from the gel network and to get hydrophobic silica aerogel and nanocomposites, the temperature ramp rate of oven is 1 °C/min.

To study the physical properties of the APD-silica aerogel nanocomposites, silylating agent/TEOS molar ratio named as HT, was varied from 2, 4, and 6 by keeping total volume of alcogel constant.

Table 1 Effect of drying temperature on the silica aerogel

Drying programmer	Aerogel density g/cm^3	Volume shrinkage%	Porosity%
100 °C × 24 h	0.248	62.2	88.7
50 °C × 5 h, 80 °C × 24 h	0.219	55.3	90.0
50 °C × 5 h, 100 °C × 24 h	0.171	38.3	92.2
50 °C × 5 h, 180 °C × 8 h	0.138	26.3	93.7
50 °C × 8 h, 80 °C × 8 h, 100 °C × 24 h, 180 °C × 8 h	0.129	22.4	94.1

Table 2 Effects of gel treatment temperature on the silica aerogel

No.	Aerogel density ρ_a/g cm^{-3}	Volume shrinkage ΔV_a/%	Wet gels treatment temperature	Sample description
1	0.289	62.7	Surface modified at 25 °C	Pieces aerogel
2	0.329	66.9	Exchanged in n-hexane at 25 °C	Pieces aerogel
3	0.171	38.3	Surface modified and exchanged at 50 °C	Bulks aerogel

2.3 Characterization

The aerogel bulk density (ρ_a) was obtained by the Archimedes method [54]. The aerogel porosity (P_a) was obtained according to the following formula:

$$P_a = \left(1 - \frac{\rho_a}{\rho_s}\right) \times 100\%$$

Wherein, ρ_s is the compact density of the silica (2.19 g/cm^3, 25 °C, 1 atm).

The shrinkage of the aerogels (ΔV_a, %) and nanocomposites (Δd_c, %) was obtained according to the following formulas:

$$\Delta V_a = \left(1 - \frac{V_{aerogel}}{V_{alcogel}}\right) \times 100\%$$

$$V_{aerogel} = \frac{m_1}{\rho_a}$$

$$\Delta d_c = \left(1 - \frac{d_c}{d_f}\right) \times 100\%$$

Wherein, $V_{alcogel}$ is the wet gel volume (cm^3), $V_{aerogel}$ is the aerogel volume (cm^3). d_c is the thickness of the nanocomposites (mm), d_f is the thickness of the microglass fiber mat (mm).

The bending strength of APD-silica aerogel nanocomposites was carried out with WDW-100 Electronic Universal Testing Machine (Bairoe), with the samples dimensions of 120 × 20 × 10 mm. The crosshead rate was 0.5 mm/min, five specimens for each kind of sample were used. The microstructure of the aerogel and nanocomposites were investigated by a Hitachi S4800 Scanning Electron Microscope (SEM) after coating the samples with a thin platinum layer. The thermal conductivities of nanocomposites were determined by a hotplate apparatus (YB/T 4130–2005) with sample dimensions of Φ180 × 20 mm. Nitrogen sorption measurements were performed to obtain pore properties with a QuadraSorb SI (Quantachrome, USA) analyzer.

3 Results and discussion

3.1 Effect of gel treatment temperature on the silica aerogel

Table 2 illustrated the wet gel treatment temperature effect on the silica aerogel. The results showed that gel treatment temperature has a significant effect on the APD-silica aerogel. The aerogel density and volume shrinkage treated at 25 °C was higher than that of 50 °C. When increasing the treatment temperature, the aerogel density decreased from 0.329 to 0.17 g/cm^3, and volume shrinkage decreased from 66.9 to 38.3%. Consequently, homogeneous and translucent bulk aerogel could be obtained at 50 °C (Fig. 2). The reasons are that the diffusivity increased at high temperature for homogeneous hydrogels according to the theory of diffusion in gels [55, 56] and the higher coarsening of the gel network occurs at 50 °C [57]. Increasing the gel treatment temperature will make a higher solvent diffusivity, a faster exchanging process, and a more absolutely replacement of end -H from Si-OH group by Si-(CH3)$_3$ group from HMDZ within the gel [49].

3.2 Effect of drying temperature on the silica aerogel

Table 1 demonstrated the effect of drying temperature on the silica aerogel. Low density and high porosity of silica

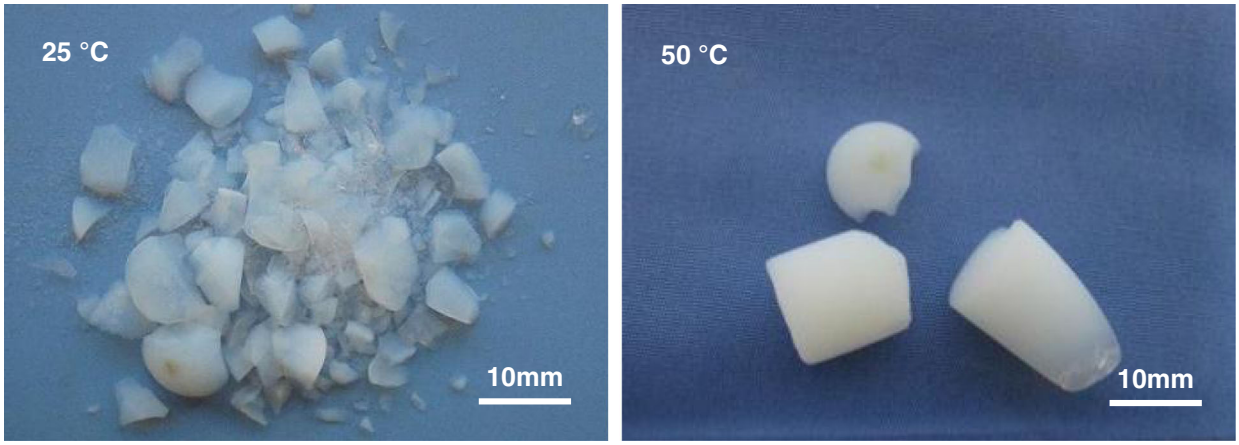

Fig. 2 Silica aerogels with different gel treatment temperature

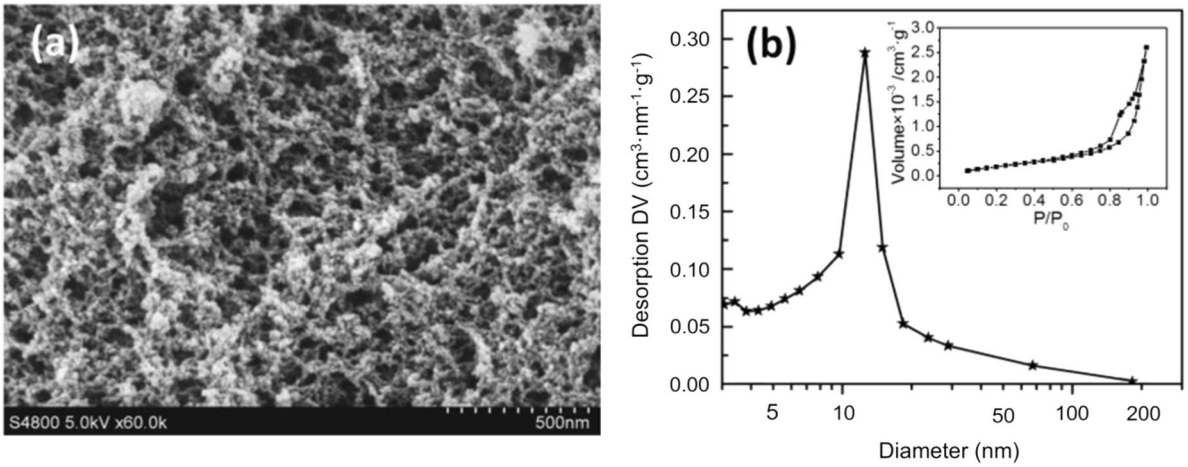

Fig. 3 SEM image **a** and pore size distribution, nitrogen adsorption isotherms **b** of retrieved APD-silica aerogel

aerogel could be obtained via APD technology with a gradient multi-segment drying process (50 °C × 8 h, 80 °C × 8 h, 100 °C × 24 h, 180 °C × 8 h), the temperature ramp rate is 1 °C/min. Lower density and volume shrinkage, higher porosity APD-silica aerogels were prepared with higher second-segment-temperature drying or gradient multi-segment drying process. The density decreased from 0.248 to 0.129 g/cm^3, and porosity increased from 88.7 to 94.1% with the gradient multi-segment drying process. The results consistent with the drying behavior of silica gels [58]. In the first drying stage named as "constant rate period", lowering drying temperature which decreasing the drying rate, solvent volatilized slowly and gel network remained well structure. If drying is too rapid, the gel body will warp or crack. In the second drying stage named as "falling rate period", the solvent surface tension and vapor pressure were reduced via gradient increasing and higher drying temperature. There is enough time for gel network to adjust its structure according to the changing of gas-liquid interface, which decreases the shrinkage and cracks of the gel.

The SEM image and pore size distribution, nitrogen adsorption isotherms of the retrieved APD-silica aerogel are shown in Fig. 3, the silica aerogel is dried with the gradient multi-segment drying process (50 °C × 8 h, 80 °C × 8 h, 100 °C × 24 h, 180 °C × 8 h). It is clear that there is uniformity and homogeneity of silica particle and porous network (Fig. 3a). According to International Union of Pure and Applied Chemistry recommendations [59], the adsorption-isotherm classification of the APD-silica aerogel (Fig. 3b) is *Type* IV isotherm, and the adsorption hysteresis is *Type* H2 loop, which is associated with capillary condensation taking place in mesopores. The specific surface area of the aerogel was 731.76 m^2/g, and the average pore size of the aerogel was 20.0 nm, smaller than that of air mean free path (66 nm, 1 atm, 23 °C) [60], it is advantageous to reduce the thermal conductivity of the aerogel. Such nano-structured particle and pores results in high

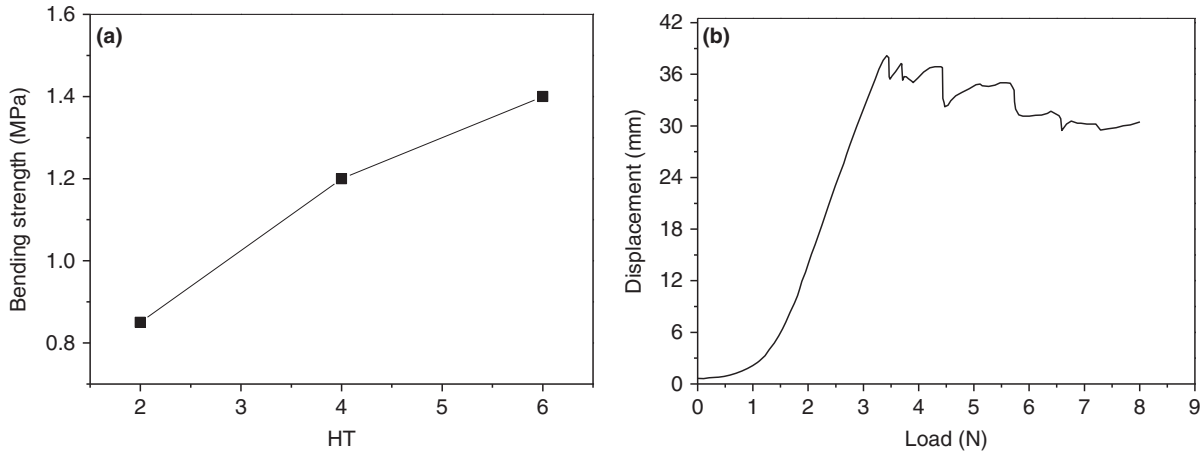

Fig. 4 Effect of HT on the bending strength **a** and the typical bending load-displacement curve **b** of the nanocomposites (HT = 6)

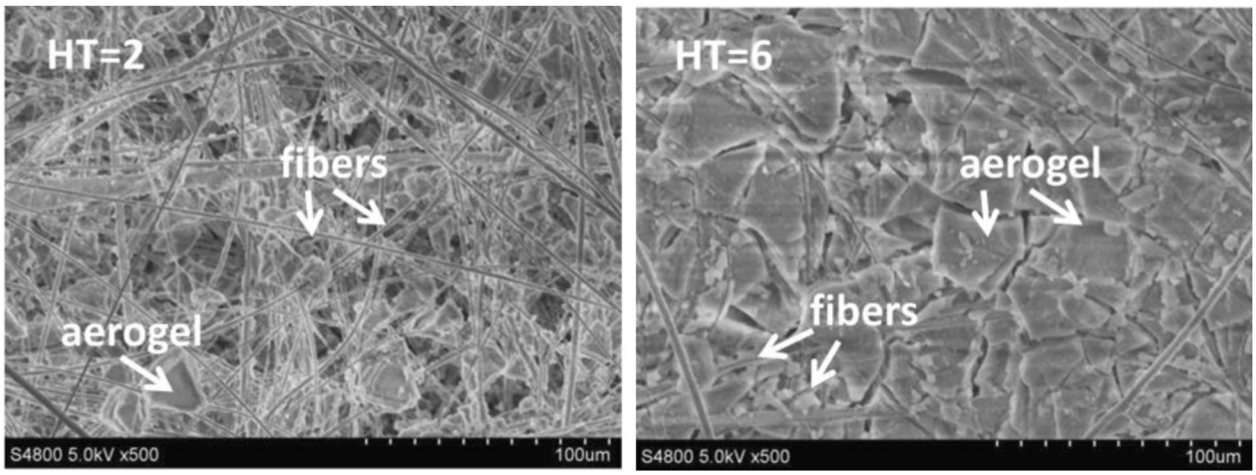

Fig. 5 SEM of nanocomposites prepared with different surface modification molar ratio (HT)

homogeneous and translucent silica aerogel (Fig. 2) with lower density (Table 1).

3.3 Effect of HT on the silica nanocomposites

Mahadik DB [61] demonstrated that by making use of surface modifying silylating reagents via TMCS and HMDZ, the apparent surface free energy of APD-silica aerogels can be tuned in a wide range from 5.5892 to 0.3073 mJ/m^2, higher concentration of silylating reagents induced lower surface free energy. Consequently, the surface polar –OH groups from wet fibers/silica gel must be replaced absolutely by non-polar –CH_3 groups, in order to get non-multi cracks nanocomposites with high mechanical performance.

As can be seen from Fig. 4a, the bending strength was improved with increasing HT, microglass fiber volume content of f_c is 9.1%. The bending strength of the nanocomposites is 1.4 MPa with the HT of six. Figure 4b shows excellent toughness of the nanocomposites with ductile fractures. The SEM of nanocomposites illustrated that fewer cracks and more silica matrix can be found with higher HT (Fig. 5). The microglass fibers adhere to the silica aerogel matrix with a stronger interface, which significantly improves the mechanical properties of the nanocomposites [62].

3.4 Effect of fibers volume content (f_c) on the silica nanocomposites

Figure 6 illustrates the effect of fibers volume content (f_c) on the thermal conductivity of nanocomposites. The thermal conductivity of the nanocomposites increased from 0.013 W/m K (200 °C) to 0.022 W/m K (650 °C) with the rise of temperature, decreased from 0.0265 W/m K (650 °C, f_c = 4.5%) to 0.022 W/m K (650 °C, f_c = 9.1%) with increasing

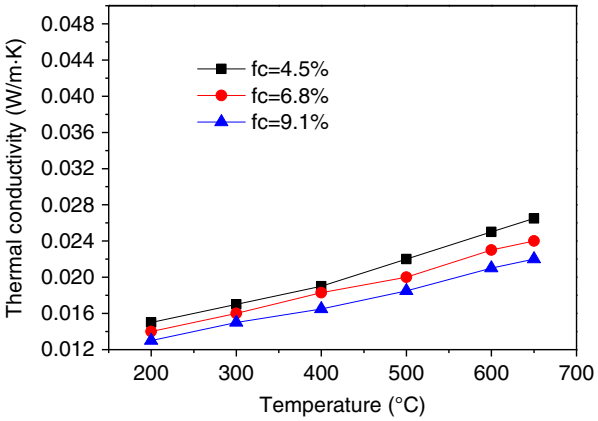

Fig. 6 Effect of fibers volume content (f_c) on the thermal conductivity of nanocomposites

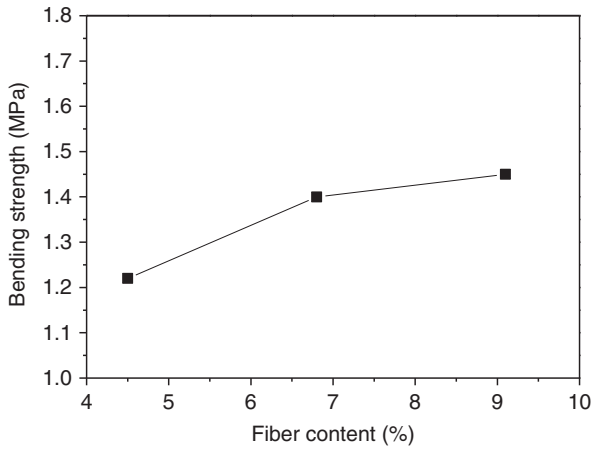

Fig. 7 Effect of fiber content on the bending strength of the nanocomposites

fiber volume content, which is lower than that of APD-silica aerogel composites strengthened with mullite fibers [40]. One of the reasons is that the retrieved nanocomposites were reinforced by microglass fibers with smaller diameters [53], results in lower radiative conductivity. Higher the fiber's volume content, higher will be the ability of depressing radiative heat conduction. Another reason is that the fibers were surrounded by APD aerogel (Fig. 4), gas convection was also depressed heavily by silica nano pore network.

On the other hand, the bending strength of the nanocomposites increased with the rising of fiber content (Fig. 7). When microglass fibers are used as the reinforcement in the nanocomposites, they received outer strength and withstand the load, and hence the higher fiber content and higher mechanical performance. Consequently, the retrieved nanocomposite is an excellent thermal insulation material with lower thermal conductivity and high mechanical performance.

4 Conclusions

A new ambient-dried silica aerogel nanocomposites reinforced by smaller diameter microglass fiber mat, with a lower thermal conductivity and high mechanical performance, was synthesized. Effects of gel treatment and drying temperature, modification agent molar ratio and microglass fibers volume content on the nanocomposites structure and properties were investigated.

Increasing the gel treatment temperature with a gradient multi-segment drying process, the aerogel density and volume shrinkage decreased rapidly. Homogeneous and translucent bulk aerogel could be obtained with the density of 0.129 g/cm^3, specific surface area of 731.76 m^2/g and average pore size of 20 nm. Fewer cracks, more silica matrix and stronger fiber/silica interface, which significantly improves the mechanical performance of the nanocomposites with the bending strength of 1.4 MPa (HT = 6). The thermal conductivity of the APD-silica aerogel nanocomposites decreased and the bending strength increased with increasing fibers volume content. The retrieved nanocomposites is an excellent thermal insulation material with lower thermal conductivity (0.022 W/m K, 650 °C, $f_c = 9.1\%$) and high mechanical performance.

Compliance with ethical standards

Conflict of interest The authors declare they have no competing interests.

References

1. Kistler SS (1931) Coherent expanded aerogels and jellies. Nature 127:741
2. Kuhn J, Gleissner T, Arduini-Schuster MC, Korder S, Fricke J (1995) Integration of mineral powders into SiO_2 aerogels. J Non-Cryst Solids 186:291–295
3. Wang J, Kuhn J, Lu X (1995) Monolithic silica aerogel insulation doped with TiO_2 powder and ceramic fibers. J Non-Cryst Solids 186:296–300
4. Lee D, Stevens PC, Zeng SQ, Hunt AJ (1995) Thermal characterization of carbon-opacified silica aerogels. J Non-Cryst Solids 186:285–290
5. Zha JJ, Duan YY, Wang XD, Zhang XR, Han YH, Gao YB, Lv ZH, Yu HT, Wang BX (2013) Optical and radiative properties of infrared opacifier particles loaded in silica aerogels for high temperature thermal insulation. Int J Therm Sci 70:54–64
6. Zhang HX, He XD, He F (2009) Microstructure and physicochemical properties of ambient-dried SiO_2 aerogels with $K_2Ti_6O_{13}$ whisker additive. J Alloy Compd 472:194–197
7. Li XK, Liu L, Zhang YX, Shen SD, Ge S, Ling LC (2011) Synthesis of nanometer silicon carbide whiskers from binary carbonaceous silica aerogels. Carbon 39:159–165
8. Fomitchev DV, Trifu R, Gould G (2004) Fiber reinforced silica aerogel composites: thermal insulation for high-temperature applications. Ninth Biennial Conference on Eng Constr Oper Challg Environ 2004:968–975

9. Gibson PW, Lee C, Ko F, Reneker D (2007) Application of nanofiber technology to nonwoven thermal insulation. J Eng Fiber Fabr 2:32–40
10. Gao QF, Feng J, Zhang CR, Feng JZ, Wu W, Jiang YG (2009) Mechanical properties of ceramic fiber-reinforced silica aerogel insulation composites. J Chin Ceram Soc 37:1–5
11. Yuan B, Ding SQ, Wang DD, Wang G, Li HX (2012) Heat insulation properties of silica aerogel/glass fiber composites fabricated by press forming. Mater Lett 75:204–206
12. Li XL, Wang QP, Li HL, Ji HM, Sun XH, He J (2013) Effect of sepiolite fiber on the structure and properties of the sepiolite/silica aerogel composite. J Sol–Gel Sci Technol 67:646–653
13. Mi CH, Jiang YG, Shi DQ, Han SW, Sun YT, Yang XG, Feng J (2014) Mechanical property test of ceramic fiber reinforced silica aerogel composites. Acta Mat Compos Sin 31:635–643
14. Jabbari M, Kesson DA, Skrifvars M, Taherzadeh MJ (2015) Novel lightweight and highly thermally insulative silica aerogel-doped poly(vinylchloride)-coated fabric composite. J Reinf Plast Comp 0:1–12
15. Karout A, Buisson P, Perrard A, Pierre AC (2005) Shaping and mechanical reinforcement of silica aerogel biocatalysts with encapsulated lipase. J Sol–Gel Sci Technol 36:163–171
16. Jones SM (2006) Aerogel: space exploration applications. J Sol–Gel Sci Technol 40:351–357
17. Shaid A, Furgusson M, Wang L (2014) Thermophysiological comfort analysis of aerogel nanoparticle incorporated fabric for fire fighter's protective clothing. Chem Mater Eng 2:37–43
18. Koebel M, Rigacci A, Achard P (2012) Aerogel-based thermal superinsulation: an overview. J Sol–Gel Sci Technol 63:315–339
19. Bheekhun N, Abu Talib AR, Hassan MR (2013) Aerogels in aerospace: an overview. Adv Mater Sci Eng 2013:1–18
20. Qi ZK, Huang DM, He S, Yang H, Hu Y, Li LM, Zhang HP (2013) Thermal protective performance of aerogel embedded firefighter's protective clothing. J Eng Fiber Fabr 8:134–139
21. Prakash SS, Brinker CJ, Hurd AJ, Rao SM (1995) Silica aerogel films prepared at ambient pressure by using surface derivatization to induce reversible drying shrinkage. Nature 374:439–443
22. Zhang HX, Qiao YJ, Zhang XH, Fang SQ (2010) Structural and thermal study of highly porous nanocomposite SiO_2-based aerogels. J Non-Cryst Solids 356:879–883
23. Jung IK, Gurav JL, Ha TJ, Choi SG, Baek S, Park HH (2012) The properties of silica aerogels hybridized with SiO_2 nanoparticles by ambient pressure drying. Ceram Int 38S:105–108
24. Yang HX, Ye F, Liu Q, Gao Y (2015) Microstructure and properties of the Si_3N_4/silica aerogel composites fabricated by the sol–gel method via ambient pressure drying. Mater Design 85:438–443
25. Han X, Williamson F, Bhaduri GA, Harvey A, Siller L (2015) Synthesis and characterisation of ambient pressure dried composites of silica aerogel matrix and embedded nickel nanoparticles. J Supercrit Fluids 106:140–144
26. Wang J, Wei Y, He WN, Zhang XT (2014) A versatile ambient pressure drying approach to synthesize silica-based composite aerogels. RSC Adv 4:51146–51155
27. Mohammadi A, Moghaddas J (2015) Synthesis, adsorption and regeneration of nanoporous silica aerogel and silica aerogel-activated carbon composites. Chem Eng Res Design 94:475–484
28. Liu HL, Chu P, Li HY, Zhang HY, Li JD (2016) Novel three-dimensional halloysite nanotubes/silica composite aerogels with enhanced mechanical strength and low thermal conductivity prepared at ambient pressure. J Sol–Gel Sci Technol 80:651–659
29. Shi YC, Li TH, Wang XL, Liu HG, Lv J, Zhang ZG (2013) Preparation and characterization of silica aerogel/mesophase pitch derived carbon foam. J Funct Mater 44:3049–3052
30. Liu HG, Li TH, Shi YC, Zhao X (2015) Thermal insulation composite prepared from carbon foam and silica aerogel under ambient pressure. J Mater Eng Perform 24:4054–4059
31. Rezaei E, Moghaddas J (2016) Thermal conductivities of silica aerogel composite insulating material. Adv Mater Lett 7:296–301
32. Chakraborty S, Pisal AA, Kothari VK, Rao AV (2016) Synthesis and characterization of fibre reinforced Silica aerogel blankets for thermal protection. Adv Mater Sci Eng 2016:1–8
33. Li Z, Cheng XD, He S, Shi XJ, Gong LL, Zhang HP (2016) Aramid fibers reinforced silica aerogel composites with low thermal conductivity and improved mechanical performance. Comp Part A 84:316–325
34. Li Z, Gong LL, Cheng XD, He S, Li CC, Zhang HP (2016) Flexible silica aerogel composites strengthened with aramid fibers and their thermal behavior. Mater Design 99:349–355
35. Martinez RG, Goiti E, Reichenauer G, Zhao SY, Koebel M, Barrio A (2016) Thermal assessment of ambient pressure dried silica aerogel composite boards at laboratory and field scale. Energ Builds 128:111–118
36. Zhang ZH, Shen J, Ni XY, Wu GM, Zhou B, Yang MX, Gu XC, Qian MJ, Wu YH (2006) Hydrophobic silica aerogels strengthened with nonwoven fibers. J Macromol Sci Part A 43:1663–1670
37. Chandradass J, Kang S, Bae DS (2008) Synthesis of silica aerogel blanket by ambient drying method using water glass based precursor and glass wool modified by alumina sol. J Non-Cryst Solids 354:4115–4119
38. Kim CY, Lee JK, Kim BI (2008) Synthesis and pore analysis of aerogel–glass fiber composites by ambient drying method. Collod Surf A 313–314:179–182
39. Shao ZD, He XY, Niu ZW, Huang T, Cheng X, Zhang Y (2015) Ambient pressure dried shape-controllable sodium silicate based composite silica aerogel monoliths. Mater Chem Phys 162:346–353
40. Liu GW, Liu YG (2016) Rapid synthesis of super insulation silica aerogel composites strengthened with mullite fibers. International Conference on Civil, Transportation and Environment (ICCTE 2016) :1300–1304
41. Zhang MC, Zeng RJ (2011) Preparation of thermal ins ulation block by slip casting and drying at ambient pressure and room temperature. J Mater Eng 9:33–38
42. Yu YX, Wu XY, San HS (2015) Preparation and characterization of hydrophobic SiO_2-glass fibers aerogels via ambient pressure drying. J Mater Eng 43:31–36
43. Motahari S, Abolghasemi A (2015) Silica aerogel–glass fiber composites as fire shield for steel frame structures. J Mater Civil Eng 27:04015008-1–7
44. Shi XJ, Zhang RF, He S, Li Z, Cao W, Cheng XD (2016) Synthesis and heat insulation performance of glass fiber reinforced SiO_2 aerogel composites. J Chin Ceram Soc 44:129–136
45. Wang BM, Song K, Ma HN (2013) Synthesis and characterization of carbon nanofibers doped silica aerogels. J Harbin Eng Univ 34:604–607
46. Ślosarczyk A, Wojciech S, Piotr Z, Paulina J (2015) Synthesis and characterization of carbon fiber/silica aerogel nanocomposites. J Non-Cryst Solids 416:1–3
47. Hayase G, Nonomura K, Kanamori K, Maeno A, Kaji H, Nakanishi K (2016) Boehmite nanofiber−polymethylsilsesquioxane core−Shell porous monoliths for a thermal insulator under low vacuum conditions. Chem Mater 28:3237–3240
48. Rao AP, Rao AV, Pajonk GM, Shewale PM (2007) Effect of solvent exchanging process on the preparation of the hydrophobic silica aerogels by ambient pressure drying method using sodium silicate precursor. J Mater Sci 42:8418–8425
49. Shewale PM, Rao AV, Rao AP (2008) Effect of different trimethyl silylating agents on the hydrophobic and physical properties of silica aerogels. Appi Surf Sci 254:6902–6907

50. Cheng Y, Li N, Wei CD (2016) Effect of the TMCS/hydrogel volume ratio on physical properties of silica aerogels based on fly ash acid sludge. J Sol–Gel Sci Technol 78:279–284
51. Rao AV, Nilsen E, Einarsrud MA (2011) Effect of precursors, methylation agents and solvents on the physicochemical properties of silica aerogels prepared by atmospheric pressure drying method. J Non-Cryst Solids 286:165–171
52. Gurav JL, Rao AV, Bangi UK (2009) Hydrophobic and low density silica aerogels dried at ambient pressure using TEOS precursor. J Alloy Compd 471:296–302
53. McKay NL, Timusk T, Farnworth B (1984) Determination of optical properties of fibrous thermal insulation. J Appli Phys 55:4064–4070
54. Bernard B, Kueppers U, Ortiz H (2015) Revisiting the statistical analysis of pyroclast density and porosity data. Solid Earth 6:869–879
55. Lauffer MA (1961) Theory of diffusion in gels. Biophys J 1:205–213
56. Amsden B (1998) Solute diffusion within hydrogels: mechanisms and models. Macromolecules 31:8382–8395
57. Scherer GW (1988) Aging and drying of gels. J Non-Cryst Solids 100:77–92
58. Simpkins PG, Johnson DW, Fleming DA (1989) Drying behavior of colloidal silica gels. J Am Ceram Soc 72:1816–1821
59. Sing KSW, Everett DH, Haul RAW, Moscou L, Pierotti RA, Rouquerol J, Siemieniewska T (1985) Reporting physisorption data for gas solid systems with special reference to the determination of surface area and porosity. Pure Appl Chem 57:603–619
60. Jennings SG (1988) The mean free path in air. J Aerosol Sci 19:159–166
61. Mahadik DB, Rao AV, Rao AP, Wagh PB, Ingale SV, Gupta SC (2011) Effect of concentration of trimethylchlorosilane (TMCS) and hexamethyldisilazane (HMDZ) silylating agents on surface free energy of silica aerogels. J Colloid Interf Sci 356:298–302
62. Feng JZ, Zhang CC, Feng J, Jiang YG, Zhao N (2011) Carbon aerogel composites prepared by ambient drying and using oxidized polyacrylonitrile fibers as reinforcements. Appl Mater Interf 3:4796–4803